AIP | Journal of Applied Physics

Geometrical dependence of spin current absorption into a ferromagnetic nanodot

Tatsuya Nomura, Kohei Ohnishi, and Takashi Kimura

Citation: Journal of Applied Physics **120**, 142121 (2016); doi: 10.1063/1.4961975
View online: http://dx.doi.org/10.1063/1.4961975
View Table of Contents: http://scitation.aip.org/content/aip/journal/jap/120/14?ver=pdfcov
Published by the AIP Publishing

Geometrical dependence of spin current absorption into a ferromagnetic nanodot

Tatsuya Nomura,[1] Kohei Ohnishi,[1,2] and Takashi Kimura[1,2,a)]
[1]Department of Physics, Kyushu University, 744 Motooka, Fukuoka 819-0395, Japan
[2]Research Center for Quantum Nano-Spin Sciences, Kyushu University, 744 Motooka, Fukuoka 819-0395, Japan

(Received 29 April 2016; accepted 18 August 2016; published online 2 September 2016)

We have investigated the absorption property of the diffusive pure spin current due to a ferromagnetic nanodot in a laterally configured ferromagnetic/nonmagnetic hybrid nanostructure. The spin absorption in a nano-pillar-based lateral-spin-valve structure was confirmed to increase with increasing the lateral dimension of the ferromagnetic dot. However, the absorption efficiency was smaller than that in a conventional lateral spin valve based on nanowire junctions because the large effective cross section of the two dimensional nonmagnetic film reduces the spin absorption selectivity. We also found that the absorption efficiency of the spin current is significantly enhanced by using a thick ferromagnetic nanodot. This can be understood by taking into account the spin absorption through the side surface of the ferromagnetic dot quantitatively. *Published by AIP Publishing.* [http://dx.doi.org/10.1063/1.4961975]

I. INTRODUCTION

Efficient manipulation of the spin current is a key ingredient for realizing next-generation spintronic devices with ultra-low electric power consumption.[1–4] Pure spin current has several advantages over the conventional spin-polarized current because of the absence of the electric current.[5–9] This leads to the suppression of the extra heat dissipation due to Joule heating, leading to the improvement of the limitation of the maximum generating spin current.[10] However, in general, the pure spin current is created by electrical spin injection in a laterally configured ferromagnetic (F)/nonmagnetic (N) metal hybrid structure. Therefore, the maximum magnitude of the pure spin current is limited by the allowable current density at the injecting F/N junction. Since most of the lateral spin valves reported so far based on ferromagnetic nanowires, which has relatively high resistivity compared to the nonmagnetic wire, a large heat dissipation due to Joule heating is generated by flowing the current. As a result, the magnitude of the spin current is restricted by the allowable maximum current density of the ferromagnetic nanowire, typically 10^8 A/cm^2 for the continuous current.[11–16]

To solve this issue, we have recently developed a different-type lateral spin valve, consisting of pillar-shaped ferromagnetic nanodots and a quasi-two-dimensional nonmagnetic film.[17,18] We showed that the Joule heating from the ferromagnetic injector is significantly suppressed in the nano-pillar-based lateral spin valve because of the reduction of the volume of the ferromagnetic element in the current probe and the efficient heat sink effect of a two dimensional nonmagnetic film. Moreover, because of its geometrical flexibility, one can easily increase the number of the spin injectors, leading to the multi-terminal spin injection. As a result, the magnitude of the generated spin current is significantly enhanced. Minimum heat dissipation under the spin injection in the nano-pillar-based lateral spin valve has been confirmed in the experiment about the spin injection into a superconductor.[19] We clearly demonstrated that the spin current was insulated at the Nb surface after the superconducting transition by using the extended nano-pillar-based lateral spin valve. It should be noted that such a spin current insulation has never been observed in the similar experiment using the nanowire-based lateral spin valve because of the reduction of the superconducting gap under the spin injection.[20,21] For realizing the efficient manipulation of the pure spin current, it is important not only to generate the spin current but also to absorb the spin current into the another ferromagnet.[22–26] However, the spin absorption efficiency in nano-pillar based lateral spin valves has not yet been evaluated. Since the large effective cross section for a two dimensional nonmagnetic film decreases the effective spin resistance of the nonmagnetic channel, the spin absorption efficiency may decrease. In the present study, we experimentally evaluate the spin current absorption efficiency in the nano-pillar-based lateral spin valve. In addition, we also explore the better structure for realizing the efficient spin absorption.

II. NANOPILLAR-BASED LATERAL SPIN VALVE

We have fabricated a nano-pillar-based lateral spin valve consisting of five ferromagnetic nanodots formed on a uniform nonmagnetic film. First, 200-nm-thick Cu and 20-nm-thick Permalloy (Py) films were deposited by electron-beam evaporation on a thermally oxidized Si substrate at the base pressure of 4×10^{-9} Torr. Subsequently, electron-beam lithography was performed to form the elliptical-shaped resist masks. The Ar ion milling process has been performed to make the Py nano-pillar structures, followed by the SiO_2 sputtering. After making the contact holes in the SiO_2 insulating layer, the top Cu electrodes were formed by the conventional lift-off process. Thus, the array of the ferromagnetic nanodots was formed on the two-dimensional uniform nonmagnetic Cu

This paper is part of the Special Topic "Cutting Edge Physics in Functional Materials" published in J. Appl. Phys. **120**, 14 (2016).

a)t-kimu@phys.kyushu-u.ac.jp.

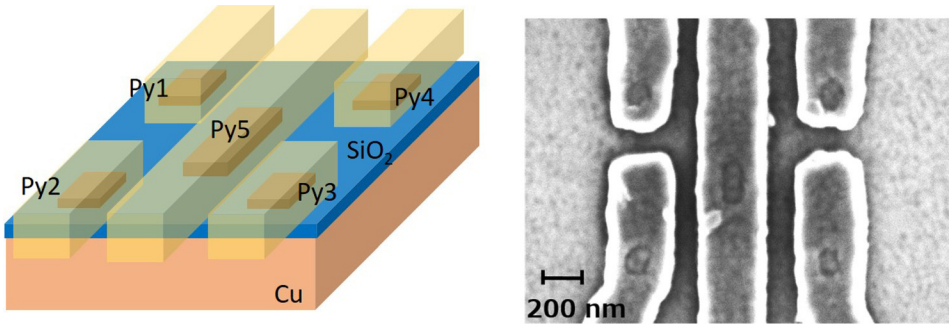

FIG. 1. Scanning electron microscopy image of the fabricated nano-pillar-based lateral spin valve with the multi spin injectors together with a schematic illustration for the fabricated lateral spin valve. The top and bottom electrodes are electrically connected via the Py nanopillars, and other regions are separated by a 100-nm-thick SiO_2 insulating layer.

film, as schematically shown in Fig. 1. Here, the desired lateral dimensions for the Py1, Py2, Py3, and Py 4, which were diagonally located on the Cu film, are approximately 120 nm × 180 nm. The desired dimension of the middle Py dot (Py5) is 120 nm × 350 nm, respectively. All the measurements in this study have been performed at 77 K. Here, the resistivity for the Py is 24 $\mu\Omega$ cm at 77 K and that for Cu is 1.6 $\mu\Omega$ cm at 77 K.

First, we evaluated the spin injection and detection efficiency for each dot by measuring the nonlocal spin valve signals, which is a barometer for the lateral spin transports, with various probe configurations. Here, we fixed the voltage probe to the middle dot (Py5). The spin injection was performed from one of the diagonally located dots (Py1, Py2, Py3, or Py4). Since the Py5 is located at the shortest distance from each ferromagnetic dot, we only consider the spin injector and detector (Py5) by neglecting the influence of the additional ferromagnetic dots. In this case, we can adapt the following basic equation for the nonlocal spin signal ΔR_S commonly used in a conventional lateral spin valve:[27]

$$\Delta R_S = \frac{P^2 R_{FI} R_{FD} R_N}{(R_N(R_{FI}+R_{FD})+2R_{FI}R_{FD})(\cosh(d/\lambda_N)+\sinh(d/\lambda_N))+R_N^2\sinh(d/\lambda)}. \quad (1)$$

Here, ΔR_S corresponds to the overall change of the nonlocal voltage divided by the excitation current. P is the spin polarization for the injector or detector. d is the center-center distance between the injector and detector. λ_N is the spin diffusion length for the nonmagnetic channel, in this case Cu. R_{FI}, R_{FD}, and R_N are the spin resistances for the injector, detector, and nonmagnetic channel. The spin resistance is defined by $2\rho\lambda/(S(1-P^2))$, where ρ and S are, respectively, the electrical resistivity and the effective cross section for the spin current.[28]

Figure 2 shows the spin valve signals for four different configurations. The nonlocal spin signals exhibit clear spin-valve effects corresponding to either parallel (high) or antiparallel (low) state. Here, the negative and positive resistance changes correspond to the magnetization reversals for the spin injector and the detector, respectively. Although the desired distance between the injector and detector is fixed to be 650 nm in all configurations, the magnitudes of the spin signals are distributed from 0.57 mΩ to 0.70 mΩ. This difference may be due to the distributions of the lateral dimensions

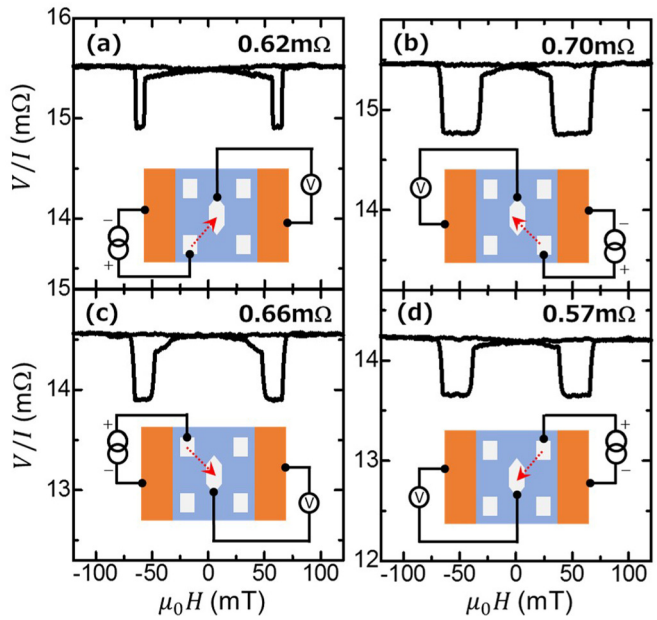

FIG. 2. Nonlocal spin valve signals by using the Py5 detector with various spin injectors measured at 77 K. The inset shows a schematic illustration of the probe configuration and the obtained spin signal.

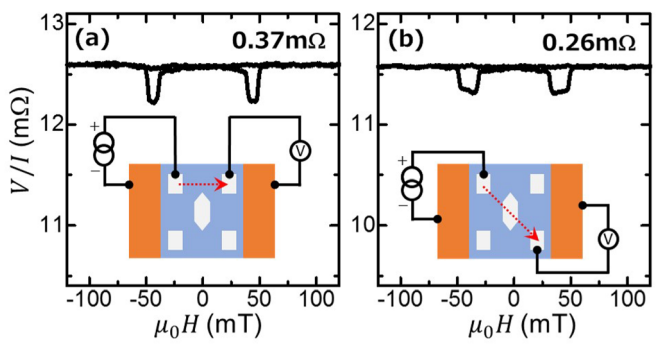

FIG. 3. (a) Nonlocal spin valve signal by using the Py1 injector and Py4 detector. (b) Nonlocal spin valve signal by using the Py1 injector and Py3 detector. Here, Py 5 is placed at the middle between Py1 and Py3.

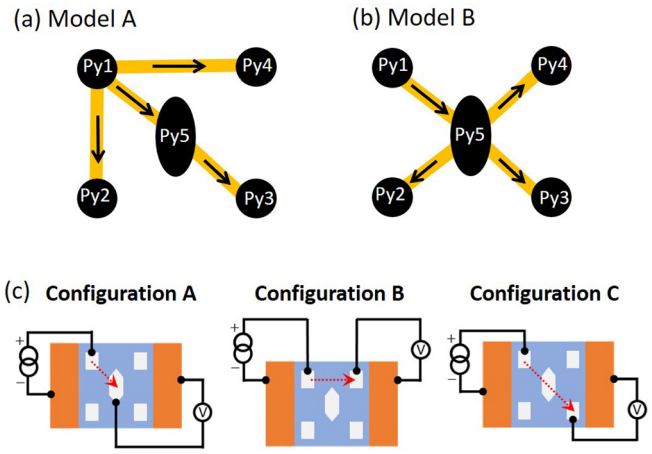

FIG. 4. Schematic illustrations for two different spin diffusion models: (a) model A and (b) model B. (c) Schematic illustrations for the representative probe configurations A, B, and C.

for the Py injectors and detectors, leading to the dispersion of the spin resistances for the injector and detector. Indeed, we can confirm from the SEM image that the Py3 has a relatively small lateral dimension compared to other Py dots. We also mention that the effective distance between the injector and detector has a small difference, leading to the distribution of the spin signal. Therefore, we believe that the distribution in the spin signals is not by the material parameters such as uniformity and interface condition but by the dispersion of the geometrical parameters in the device.

In the above analysis, we neglected the influence of the other ferromagnetic dots on the spin current distribution. However, the obtained spin signal was smaller than the previously reported device with a similar lateral dimension.[17] This is because the spin current distribution is affected by other ferromagnetic dots. To clarify the influence of the multi spin injectors and analyze the spin absorption efficiency due to the Py5, we evaluate the nonlocal spin valve signal with various probe configurations. Here, we compare the nonlocal spin valve signals between two configurations. One is the nonlocal spin valve measurement using Py1 and Py4 and the other one is that using Py 1 and Py 3. Here, it should be noted that in the latter configuration, a middle ferromagnetic dot (Py5) is located in between Py1 and Py4. Therefore, we expect that the significant reduction of the spin signal is expected because of the spin current absorption effect into Py5. As in Fig. 3(a), the obtained spin signal using Py1 and Py4 is 0.37 mΩ, which is smaller than the value expected from the previous nanopillar lateral spin valve.[17] Moreover, as in Fig. 3(b), we obtain 0.26 mΩ, which is comparable to the spin signal in Fig. 3(a) although a spin absorber is located at the center of the injector and detector. These results imply that the spin current absorption exists in both configurations.

To survey the probe-configuration dependence of the spin signal, we propose two different models based on the one dimensional spin diffusion model.[29] In the first model (model A), we consider the spin absorption effect only in the spin current diffusion along the diagonal direction, as conceptually shown in Fig. 4(a). Here, we neglect the influence of the middle spin absorber on the spin diffusion to Py2 and Py3. In this case, by using $\rho_{Py}\lambda_{Py}/\rho_{Cu}\lambda_{Cu} = 0.2$, which is approximately equal to the ratio of the spin resistance for the ferromagnetic dot to that for the nonmagnetic Cu film,[27] we can calculate the spin signals $\Delta R_S^A, \Delta R_S^B$, and ΔR_S^C for the configurations A, B, and C shown in Fig. 4(c). From the calculation, we obtained the following relationship of the spin signals:

$$\Delta R_S^B = 1.41\Delta R_S^A, \quad \Delta R_S^C = 0.25\Delta R_S^A.$$

Although the second relationship is reasonable, the first relationship is quite far from the experimental result, indicating invalid situation of the proposed model. To improve these discrepancies, we proposed another model (model B), in which we consider the spin absorption effect due to the middle Py dot for all branches. By using the same values of $\rho_{Py}\lambda_{Py}/\rho_{Cu}\lambda_{Cu}$ as in model A, we obtain the following relationship for the spin signals:

$$\Delta R_S^B = 0.65\Delta R_S^A, \quad \Delta R_S^C = 0.32\Delta R_S^A.$$

These values show reasonable consistency with the experimental results, indicating that the middle ferromagnetic dot acts as a good spin absorber even in the nanopillar-based lateral spin valve because of its large lateral dimension of the Py dot. However, because of the small spin resistance of the quasi-two-dimensional Cu film, the absorption efficiency is smaller than the conventional lateral spin valve.[30]

III. SPIN CURRENT ABSORPTION THROUGH SIDE SURFACE

In order to increase the spin absorption efficiency, the spin resistance for the spin absorber should be much smaller than the spin resistance for the nonmagnetic channel. Since the spin resistance is inversely proportional to the cross section, increasing the effective cross section is one of the ways for improving the absorption efficiency.[28] By increasing the lateral dimension of the F dot or F/N junction size, one can reduce the spin resistance for the spin absorber.[24] Indeed, in

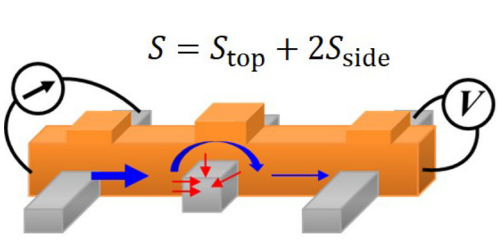

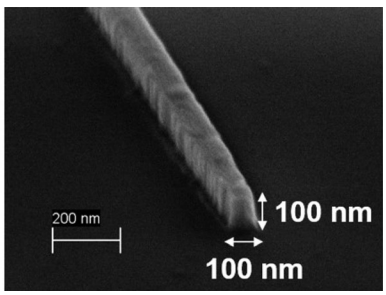

FIG. 5. Schematic illustration for the spin absorption measurement together with the cross-sectional SEM image of the 100-nm-thick Py nanowire.

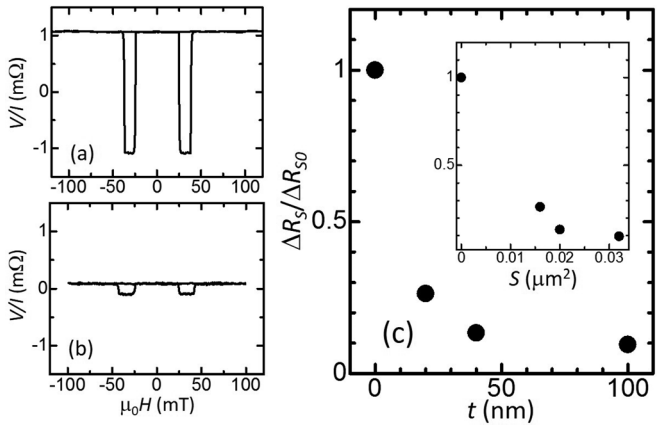

FIG. 6. Spin absorption effect in a conventional lateral spin valve. Nonlocal spin valve signal (a) without and (b) with the 100-nm-thick Py dot. (c) Reduction of the spin valve signal as a function of the dot thickness. The inset of (c) is the reduction of the spin valve signal as a function of the effective junction size of the spin absorber.

the experiment of Sec. II, we showed that the spin current was effectively absorbed into the ferromagnetic dot with a large lateral dimension. However, increasing the lateral dimension does not improve the density of the spin current and is not suitable for nano-sized spin devices from the view point of the device integration. To improve the absorption efficiency, we focus on the spin absorption from the side surface, which is another way for increasing the effective cross section for the spin current.

To investigate the spin current absorption from the side surface, we have fabricated the lateral spin valves with middle ferromagnetic dots with different dot thicknesses, as schematically shown in Fig. 5. Here, we have prepared 20-, 40-, and 100-nm-thick ferromagnetic middle dots. We believe that the side surface of the thick ferromagnetic dot was cleaned by the conventional Ar ion milling because of the forward tapered cross section of the ferromagnetic dot as shown in Fig. 5(b). In addition, the deposition rate of the Cu was 0.5 nm/s to obtain a better surface covering around the Py dot.

The absorption efficiency for each device has been evaluated by comparing the spin signal to that without the middle absorber. Figures 6(a) and 6(b) show the typical results of the spin current absorption. We have clearly observed the significant reduction of the spin signal. Moreover, as can be seen in Fig. 6(c), it was confirmed that the reduction of the spin signal increases by increasing the dot thickness. This implies that the side surface of the middle ferromagnet acts as an efficient spin absorber.[24,25] To clarify the influence of the spin absorption from the side surface, we replot the ratio of the spin signal as a function of the effective cross section in the inset of Fig. 6(c). Here, the effective cross section is the sum of the top surface and two side surface areas. A large reduction of the spin signal was observed at $S \approx 0.02\,\mu m^2$. To understand this behavior, we may have to take into account the influence of the geometrical disorder, which may induce the additional spin-flip scattering, when the thickness of the middle ferromagnetic dot increases. However, since the influence of the geometrical scattering also increases with increasing the thickness, we cannot distinguish the origin of the reduction.

To exclude the influence of the geometrically induced scattering, we have developed a modified lateral spin valve consisting of a T-shaped Cu channel shown in Fig. 7. Here, the spin absorber is placed under the branch of the Cu channel. Therefore, the spin current diffusing into the Py detector is not affected by the geometrical disorder of the spin absorber. Here, we have fabricated the modified lateral spin valves with the different dot thicknesses, 10, 30, 60, 80, and 100 nm. The spin absorption efficiency is evaluated from the comparison of the spin signal with and without the ferromagnetic dot.

Figures 8(a) and 8(b) show the spin signals with and without the ferromagnetic absorber, respectively. Here, the spin signal without the absorber is slightly smaller than that in Fig. 6(a), indicating that the influence of the additional Cu branch is small in the spin diffusion in the Cu channel. However, we have clearly observed the reduction of the spin signal in Fig. 8(b) by putting the Py dot in the branch because of the spin absorption effect. Moreover, as shown in Fig. 8(c), the spin signal monotonically decreases by increasing the dot thickness. This is a strong evidence that the pure spin current is efficiently absorbed from the side surface of the ferromagnetic dot similarly to the top surface.

Here, we analyze the spin absorption efficiency in the modified lateral spin valve. Based on the one dimensional spin diffusion model, the spin signal ΔR_S with the middle absorber can be approximately calculated as follows:[27,28]

$$\Delta R_S \approx \frac{\left(PR^S_{\mathrm{Py}}\right)^2 R^S_{\mathrm{Abs}}}{R^S_{\mathrm{Cu}}\left(R^S_{\mathrm{Cu}}(1-\cosh(d/\lambda_{\mathrm{Cu}})) + 2\left(R^S_{\mathrm{Py}} + R^S_{\mathrm{Abs}}\right)\sinh(d/\lambda_{\mathrm{Cu}})\right)}, \tag{2}$$

where R^S_{Py}, R^S_{Cu}, and R^S_{Abs} are the spin resistances for Py, Cu, and the middle spin absorber, respectively. P is the spin polarization for the Py. d is the distance between the injector and detector. It should be noted that in this kind of lateral spin valve based on the metallic wires, R^S_{Cu} is much larger than R^S_{Abs} and R^S_{F}. Since the spin absorber is placed in the Cu branch at a small distance from the intersection, we neglect the spin relaxation in the Cu branch. In order to consider the

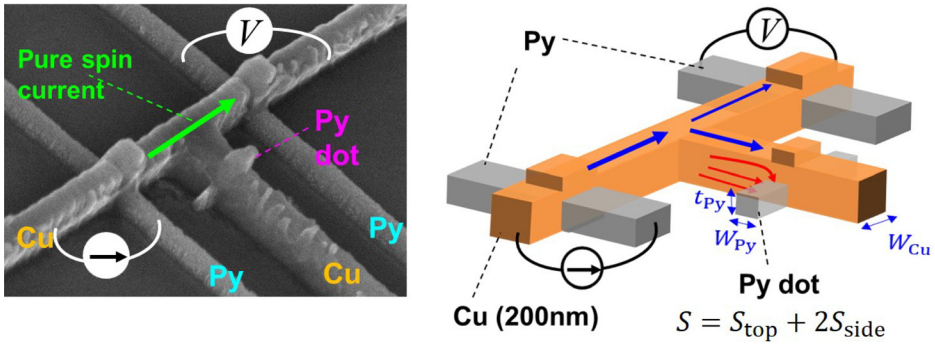

FIG. 7. Scanning electron microscopy image of the modified lateral spin valve together with the schematic illustration of the fabricated device.

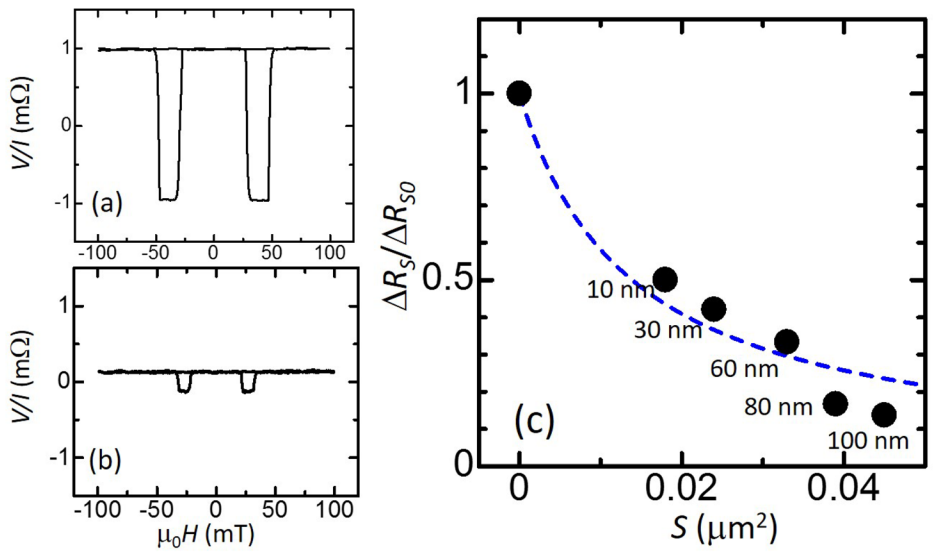

FIG. 8. Spin absorption effects in a modified lateral spin valve. Nonlocal spin valve signal (a) without and (b) with the 100-nm-thick Py dot. (c) Reduction of spin valve signal as an effective junction size of the Py-dot.

influence of the absorber thickness, we assume that the effective cross section for the spin resistance is given by $S_{top} + 2S_{side}$, where S_{side} is $w_{Cu}t_{dot}$, as schematically shown in the inset of Fig. 8(c). Using the above assumption, we tried to reproduce the reduction of the spin signal observed in Fig. 8. The fitted curve roughly reproduces the experimental results. However, the reduction rate significantly increases at $t > 80$ nm. The reason for this deviation is unclear at the moment but further reduction from the theoretical calculated value indicates that the side surface is an efficient current absorber for the diffusive spin current. It should also be mentioned that the expanded one-dimensional spin resistor model may be useful for more quantitative understanding.[25,31]

IV. CONCLUSION

We have investigated the spin absorption properties in nano-pillar-based and nanowire-based multi-terminal lateral spin valves. Although the spin absorption efficiency in the nano-pillar-type device was smaller than that in the conventional wire-type device, the absorption rate in the nano-pillar device was increased by increasing the junction size similarly in the conventional devices. However, the spin absorber had to have a large lateral dimension in order to maintain the large spin absorption efficiency. To obtain a large spin absorption efficiency with a small lateral dimension, we proposed the spin absorption effect from the side surfaces of a thick ferromagnetic dot. In order to evaluate the spin absorption efficiency through the side surface properly, a modified lateral spin valve with a T-shaped nonmagnetic wire has been proposed. We clearly demonstrated that the spin absorption from the side surface was consistently enhanced by increasing the junction area of the side surface.

ACKNOWLEDGMENTS

This work was partially supported by Grant-in-Aid for Scientific Research on Innovative Area, "Nano Spin Conversion Science" (26103002), that for Challenging Exploratory Research (26630162) and that for Scientific Research (S) (25220605).

[1]I. Zutić, J. Fabian, and S. Das Sarma, Rev. Mod. Phys. **76**, 323 (2004).
[2]*Concepts in Spin Electronics*, edited by S. Maekawa (Oxford University Press, 2006).
[3]*Spin Current*, edited by S. Maekawa *et al.* (Oxford University Press, 2012).
[4]*Handbook of Spin Transport and Magnetism*, edited by E. Y. Tsymbal and I. Zutic (CRC, 2011).
[5]M. Johnson and R. H. Silsbee, Phys. Rev. Lett. **55**, 1790 (1985).
[6]F. J. Jedema, A. T. Filip, and B. J. van Wees, Nature **410**, 345 (2001).
[7]S. O. Valenzuela, Int. J. Mod. Phys. B **23**, 2413 (2009).
[8]T. Kimura and Y. Otani, J. Phys.: Condens. Matter **19**, 165216 (2007).
[9]A. Hoffmann, Phys. Status Solidi C **4**(11), 4236 (2007).
[10]S. Nonoguchi, T. Nomura, Y. Ando, and T. Kimura, J. Appl. Phys. **111**, 07C505 (2012).
[11]A. Yamaguchi *et al.*, Phys. Rev. Lett. **92**, 077205 (2004).
[12]G. S. D. Beach *et al.*, Phys. Rev. Lett. **97**, 057203 (2006).
[13]M. Hayashi *et al.*, Phys. Rev. Lett. **97**, 207205 (2006).

[14]M. Klaui *et al*., Phys. Rev. Lett. **95**, 026601 (2005).
[15]G. Meier *et al*., Phys. Rev. Lett. **98**, 187202 (2007).
[16]T. Kimura, Y. Otani, I. Yagi, K. Tsukagoshi, and Y. Aoyagi, J. Appl. Phys. **94**, 7947–7949 (2003).
[17]S. Nonoguchi, T. Nomura, and T. Kimura, Appl. Phys. Lett. **100**, 132401 (2012).
[18]S. Bakaul, S. Hu, and T. Kimura, Appl. Phys. A **111**, 355–360 (2013).
[19]K. Ohnishi, T. Ono, T. Nomura, and T. Kimura, Sci. Rep. **4**, 6260 (2014).
[20]N. Poli *et al*., Phys. Rev. Lett. **100**, 136601 (2008).
[21]T. Wakamura, N. Hasegawa, K. Ohnishi, Y. Niimi, and Y. Otani, Phys. Rev. Lett. **112**, 036602 (2014).
[22]T. Kimura, Y. Otani, and J. Hamrle, Phys. Rev. Lett. **96**, 037201 (2006).
[23]T. Yang, T. Kimura, and Y. Otani, Nat. Phys. **4**, 851 (2008).
[24]T. Kimura, Y. Otani, and J. Hamrle, Phys. Rev. B **73**, 132405 (2006).
[25]P. Laczkowski *et al*., Phys. Rev. B **92**, 214405 (2015).
[26]Y. Niimi and Y. Otani, Rep. Prog. Phys. **78**, 124501 (2015).
[27]S. Takahashi and S. Maekawa, Phys. Rev. B **67**, 052409 (2003).
[28]T. Kimura, J. Hamrle, and Y. Otani, Phys. Rev. B **72**, 014461 (2005).
[29]O. Stejskala, J. Hamrle, J. Pistora, and Y. Otani, J. Magn. Magn. Mater. **414**, 132–143 (2016).
[30]E. Masourakis *et al*., Nanotechnology **27**, 095201 (2016).
[31]W. S. Torres *et al*., e-print arXiv:1506.01347.